

# Spin-Orbit Qubit on a Multiferroic Insulator in a Superconducting Resonator

P. Zhang,<sup>1</sup> Ze-Liang Xiang,<sup>1</sup> and Franco Nori<sup>1,2</sup>

<sup>1</sup>*Center for Emergent Matter Science, RIKEN, Saitama 351-0198, Japan*

<sup>2</sup>*Department of Physics, The University of Michigan, Ann Arbor, Michigan 48109-1040, USA*

(Dated: November 14, 2018)

We propose a spin-orbit qubit in a nanowire quantum dot on the surface of a multiferroic insulator with a cycloidal spiral magnetic order. The spiral exchange field from the multiferroic insulator causes an inhomogeneous Zeeman-like interaction on the electron spin in the quantum dot, producing a spin-orbit qubit. The absence of an external magnetic field benefits the integration of such spin-orbit qubit into high-quality superconducting resonators. By exploiting the Rashba spin-orbit coupling in the quantum dot via a gate voltage, one can obtain an effective spin-photon coupling with an efficient on/off switching. This makes the proposed device controllable and promising for hybrid quantum communications.

PACS numbers: 81.07.Ta, 71.70.Ej, 75.85.+t

## I. INTRODUCTION

Spin-based qubits, owing to their long coherence times and individual coherent manipulation, are promising candidates for building blocks of quantum information processors.<sup>1–5</sup> A conventional spin qubit can be simply realized via Zeeman splitting of two Kramers-degenerate states by a static magnetic field and controlled by an ac magnetic field.<sup>2,6–8</sup> However, its application is limited due to the difficulty in generating and localizing an ac magnetic field at the nanoscale. Owing to the interplay between spin and orbital degrees of freedom, the spin-orbit qubit allows the possibility for manipulating spins via an easily-accessible ac electric field, i.e., by means of the electric-dipole spin resonance (EDSR).<sup>9,10</sup> Intuitively, the interplay between spin and orbit can arise from the spin-orbit coupling (SOC), e.g., the Rashba or Dresselhaus type, which couples the electron spin  $\sigma$  to the momentum  $\mathbf{p}$ . The SOC-mediated EDSR has been widely studied in the literature.<sup>11–18</sup> Instead of invoking SOC, an alternative way to achieve the interplay between spin and orbit is coupling the electron spin  $\sigma$  to the coordinate  $\mathbf{r}$ . This spin-coordinate coupling can be accomplished by, e.g., an inhomogeneous Zeeman-like interaction<sup>15,19–23</sup> or a fluctuating hyperfine interaction.<sup>24,25</sup>

Apart from coherent manipulation, scaling up the spin-orbit-qubit architecture also involves quantum information storing and transferring. Embedding the spin-orbit qubit into a cavity resonator to achieve spin-photon coupling seems particularly attractive, as the mobile photons in the cavity can store and transfer quantum information with little loss of coherence.<sup>26</sup> Indeed, in view of their energy scales, the semiconductor-based spin-orbit qubit is compatible with the superconducting microwave resonator. Moreover, integrating the spin-orbit qubit into the superconducting cavity promotes hybrid quantum communications, e.g., in combination with superconducting qubits or charge qubits.<sup>26–28</sup> Several proposals for coupling spin-orbit qubits to superconducting cavities have been reported.<sup>15,23,29,30</sup> However, the spin-orbit qubit invoking SOC requires an external static mag-

netic field,<sup>12,13,16,18</sup> which is not naturally compatible with superconducting cavities of high quality factors.<sup>23</sup> Therefore, a spin-orbit qubit without an external magnetic field is preferred for constructing a hybrid system. It has been proposed that, by using an inhomogeneous Zeeman-like interaction induced by ferromagnetic contacts or micromagnets,<sup>20–23</sup> one can realize spin-orbit qubits in the absence of a magnetic field and effectively couple them to superconducting cavities.<sup>15,23</sup>

In this work, we propose a spin-orbit qubit mediated by the spin-coordinate coupling and study its coupling to a superconducting coplanar waveguide resonator. Different from previous studies,<sup>15,19–25</sup> our proposal relies on the inhomogeneous exchange field arising from the multiferroic insulators with a cycloidal spiral magnetic order.<sup>31–36</sup> These multiferroic insulators provide a unique opportunity for the design of functional devices owing to the cycloidal spiral magnetic order as well as the magnetoelectric coupling.<sup>36–38</sup> In our setup for the spin-orbit qubit, as illustrated in Fig. 1(a), a gated nanowire with a quantum dot is placed on top of a multiferroic insulator. The spiral exchange field arising from the magnetic moments in the multiferroic insulator causes an inhomogeneous Zeeman-like interaction on the quantum-dot spin. Therefore, a spin-orbit qubit is produced in the nanowire quantum dot. The absence of an external magnetic field facilitates the integration of the spin-orbit qubit into the superconducting coplanar waveguide, as illustrated in Fig. 1(b). In this hybrid circuit, both the level spacing of the spin-orbit qubit and the spin-photon coupling depend on the ratio between the dot size and the wavelength of the spiral magnetic order in the substrate. When the Rashba SOC is introduced into the nanowire, the level spacing and spin-photon coupling can be adjusted by tuning the Rashba SOC via a gate voltage on the nanowire. With the modulation of the Rashba SOC, we can obtain an effective spin-photon coupling with an efficient on/off switching. This is promising for manipulating, storing and transferring quantum information in the data bus provided by the circuit cavity.

This paper is organized as follows. First, we establish

the spin-orbit qubit on the surface of a multiferroic insulator. After that, we integrate the spin-orbit qubit into a superconducting coplanar waveguide and study its spin-photon coupling. We further study the modulation of the Rashba SOC on the hybrid system. At last we discuss the experimental realizability of the proposed device.

## II. SPIN-ORBIT QUBIT ON A MULTIFERROIC INSULATOR

Our study starts from the device schematically shown in Fig. 1(a). In this setup, a nanowire lies on the surface of a multiferroic insulator, e.g., TbMnO<sub>3</sub> or BiFeO<sub>3</sub>,<sup>31,33–36</sup> and is aligned parallel to the propagation direction of the spiral magnetic moments in the substrate. The nanowire is gated by two electrodes producing a quantum dot, which is assumed to be subject to a 1D parabolic potential.

We consider a single electron in the quantum dot. In the coordinate system with the  $x$ -axis along the nanowire and the  $z$ -axis perpendicular to the top surface of the multiferroic insulator, the electron is described by the Hamiltonian,

$$H = \frac{p^2}{2m_e} + \frac{1}{2}m_e\omega^2x^2 + \mathbf{J}(x) \cdot \boldsymbol{\sigma}. \quad (1)$$

Here  $m_e$  is the effective electron mass and  $p = -i\hbar\partial_x$  is the momentum operator. The second term in the Hamiltonian is the parabolic potential. The last term depicts the interaction between the electron spin  $\boldsymbol{\sigma}$  and the exchange field from the cycloidal spiral magnetic moments,

$$\mathbf{J}(x) = J(\sin(\chi qx + \phi), 0, \cos(\chi qx + \phi)). \quad (2)$$

In writing this term we have assumed the dot size  $x_0 = \sqrt{\hbar/(m_e\omega)}$  to be much larger than the distance ( $\sim 0.1$  nm) between the nearby magnetic atoms in the substrate. Here  $q = 2\pi/\lambda$  is the wavevector of the spiral order corresponding to a wavelength  $\lambda$  and  $\phi$  ( $0 \leq \phi < 2\pi$ ) is the phase of the exchange field at  $x = 0$ . The spiral helicity  $\chi$  ( $= \pm 1$ ) of the magnetic order is reversible by a gate voltage on the multiferroic insulator [as illustrated by  $V_c$  in Fig. 1(a)] due to the magnetoelectric coupling.<sup>33</sup> The strength of the exchange coupling  $J$  (we assume  $J > 0$ ) between the electron spin and the magnetic moments, depending on their distance and the specific hosts, is weak and assumed to be of the order of 1-10  $\mu\text{eV}$ .<sup>20,23</sup>

Due to the spiral geometry of the magnetic order, the macroscopic magnetism of the multiferroic insulator is zero, while the exchange coupling still breaks the time-reversal symmetry locally and causes an inhomogeneous Zeeman-like interaction on the quantum-dot spin. In the presence to this inhomogeneous Zeeman-like interaction, a spin-orbit qubit is realizable in the quantum dot. One can also understand the availability of a spin-orbit qubit in our setup in the spiral frame with

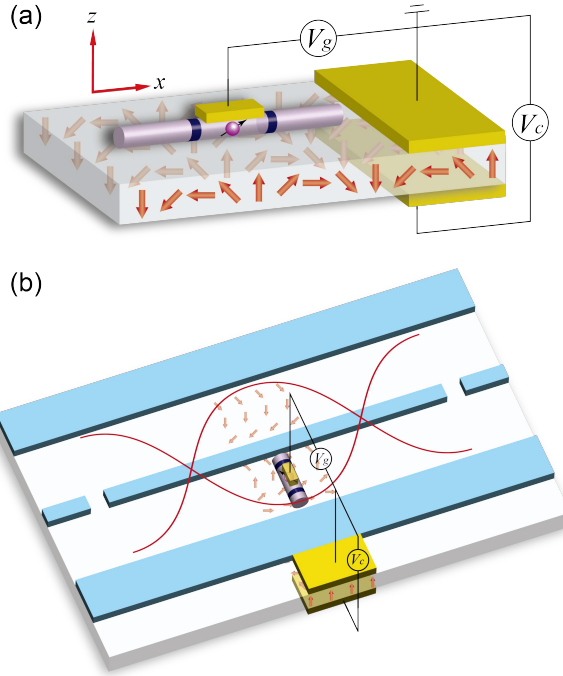


FIG. 1: (Color online) (a) Schematic of the proposed spin-orbit qubit: a gated nanowire on the surface of a multiferroic insulator. The nanowire is aligned along the propagation direction of the spiral magnetic order in the multiferroic insulator, indicated by the series of rotating arrows. Two gate electrodes (indicated by the two dark blue ring-shaped contacts) supply a parabolic confining potential and form a quantum dot in between. The gate electrode on the top of the quantum dot with voltage  $V_g$  controls the Rashba SOC. Two gate electrodes on the top and bottom of the multiferroic insulator supply a voltage  $V_c$  which controls the spiral helicity of the magnetic order. (b) Schematic of the integration of the spin-orbit qubit into a superconducting coplanar waveguide resonator. The nanowire is placed parallel to the electric field between the center conductor and the ground plane and located at the maximum of the electric field. Note that in the multiferroic-insulator substrate, only the magnetic moments near the nanowire are schematically shown by the rotating arrows.

the spin  $z$ -axis along the local magnetic moment. Using a unitary transformation  $\tilde{H} = U^\dagger(x)H U(x)$ , where  $U(x) = \exp[-i(\chi qx + \phi)\sigma_y/2]$ ,<sup>37</sup> one arrives at

$$\tilde{H} = \frac{p^2}{2m_e} + \frac{1}{2}m_e\omega^2x^2 - \alpha_0 p\sigma_y + J\sigma_z + \frac{\hbar^2 q^2}{8m_e}, \quad (3)$$

where  $\alpha_0 = \chi\hbar q/(2m_e)$ . This Hamiltonian evidently indicates that in the spiral frame, the exchange field supplies not only the homogeneous Zeeman-like interaction,  $J\sigma_z$ , but also an effective Rashba-like SOC,  $-\alpha_0 p\sigma_y$ .<sup>37</sup> This Hamiltonian is equivalent to the one studied in Ref. 16, where a spin-orbit qubit was realized by virtue of an external magnetic field and the genuine Rashba/Dresselhaus SOC.

Now we demonstrate the realization of a spin-orbit

qubit by studying the low-energy bound states in the quantum dot. For the reasonable case with  $J/(\hbar\omega) \lesssim 0.1$ , the exchange coupling can be treated as a perturbation. We rewrite the Hamiltonian (1) as  $H = H_0 + H_1$ , where  $H_1 = \mathbf{J}(x) \cdot \boldsymbol{\sigma}$ . The eigenstates of  $H_0$ , describing a harmonic oscillator, can be written as  $|n\pm\rangle = |n\rangle|\pm\rangle$  with the eigenenergies  $\varepsilon_n = (n + \frac{1}{2})\hbar\omega$  ( $n = 0, 1, 2, \dots$ ). Here  $|n\rangle$  is the orbital eigenstate of the harmonic oscillator and  $|+\rangle$  ( $|-\rangle$ ) is the spin-up (-down) eigenstate of  $\sigma_z$ . We focus on the  $n = 0$  Hilbert subspace which is two-fold degenerate. First-order degenerate perturbation theory gives the lowest two bound states of  $H$  with energies  $\varepsilon_{0\pm} = \varepsilon_0 \pm \hbar\Delta/2$ , where

$$\Delta = \Delta_0 \exp(-\eta^2), \quad (4)$$

with  $\Delta_0 = 2J/\hbar$  and  $\eta = \chi\pi x_0/\lambda$ . The corresponding wavefunctions are

$$\begin{aligned} |\widetilde{0\pm}\rangle = & e^{-i\phi\sigma_y/2} \left\{ |0\pm\rangle - \frac{Je^{-\eta^2}}{\hbar\omega} \sum_{m=1}^{+\infty} \left[ \frac{\pm(i\sqrt{2}\eta)^{2m}}{2m\sqrt{(2m-1)!}} |2m\pm\rangle \right. \right. \\ & \left. \left. - \frac{i(i\sqrt{2}\eta)^{2m-1}}{(2m-1)\sqrt{(2m-1)!}} |2m-1\mp\rangle \right] \right\}. \end{aligned} \quad (5)$$

The two lowest bound states  $|\widetilde{0\pm}\rangle$ , spaced by  $\hbar\Delta$  and about  $\hbar\omega$  away from the nearest higher-energy state, can be used to encode the spin-orbit qubit. As a result, with the aid of the spiral exchange field supplied by a multiferroic insulator, we realize a spin-orbit qubit in the absence of an external magnetic field as well as the Rashba/Dresselhaus SOC.

### III. SPIN-PHOTON COUPLING IN A SUPERCONDUCTING CAVITY

The spin-orbit qubit can respond to an ac electric field, via EDSR.<sup>9,10</sup> Due to the small level spacing, the spin-orbit qubit is controllable by low-temperature microwave technology. This can be accomplished by virtue of a superconducting resonator, which works at temperatures  $\sim$  mK with resonance frequencies  $\sim$  GHz.<sup>26</sup> Indeed, integrating spin-orbit qubits into superconducting resonators has recently attracted much interest,<sup>15,23,29,30</sup> to explore novel hybrid quantum circuits.<sup>26</sup> Moreover, the spin-orbit qubit proposed here, which is external-magnetic-field-free, is naturally compatible with superconducting resonators of high quality factors.

As schematically shown in Fig. 1(b), we embed the spin-orbit qubit into a superconducting coplanar waveguide,<sup>15,26</sup> with the nanowire aligned parallel to the electric field between the center conductor and the ground plane. The resonant photon energy ( $\sim$  GHz) is too low to excite magnons in the multiferroic-insulator substrate,<sup>35</sup> and we assume that the spiral magnetic order keeps steady during the operation of the spin-orbit qubit. The spin-orbit qubit, photons, as well as their

coupling, can be described by the Hamiltonian,<sup>26</sup>

$$H_{\text{eff}} = \frac{\hbar\Delta}{2} s_z + \hbar\omega_r \left( a^\dagger a + \frac{1}{2} \right) + \hbar g (a^\dagger s_- + a s_+). \quad (6)$$

Here  $a$  ( $a^\dagger$ ) is the annihilation (creation) operator for photons with frequency  $\omega_r$  in the cavity, and  $s_{x,y,z}$  are the Pauli matrices in the  $|\widetilde{0\pm}\rangle$  subspace with  $s_\pm = (s_x \pm is_y)/2$ . The spin-photon coupling strength

$$g = \langle \widetilde{0+} | x | \widetilde{0-} \rangle E e/\hbar, \quad (7)$$

where  $E$  is the cavity electric field on the spin-orbit qubit. Up to first order in  $J/(\hbar\omega)$ ,

$$g = g_0 (x_0/\lambda)^3 \eta \exp(-\eta^2), \quad (8)$$

where  $g_0 = -eEm_eJ\lambda^3/\hbar^3$ .

Note that in this device, both the level spacing  $\Delta$  and the spin-photon coupling  $g$  are independent of the phase  $\phi$  and proportional to the exchange coupling strength  $J$ . Also, both  $\Delta$  and  $g$  strongly depend on the ratio between the dot size  $x_0$  and the wavelength  $\lambda$  of the spiral magnetic order. In Fig. 2, we plot the dependence of  $\Delta/\Delta_0$  and  $|g/g_0|$  on the parameter  $x_0/\lambda$ . One finds that when  $x_0/\lambda$  is close to 1, both  $\Delta$  and  $|g|$  approach zero, hindering the device operation. This is because when  $x_0/\lambda$  is large, the exchange field, oscillating with a high frequency in the scale of the dot size, has quite small matrix elements between the  $|n\pm\rangle$  and  $|n'\pm\rangle$  states. This leads to a vanishing Zeeman-like splitting and spin-orbit mixing of the harmonic oscillator states. However, in the  $x_0/\lambda = 0$  limit,  $\Delta$  reaches its maximum while  $|g|$  again approaches zero. In fact, in this regime, with the approximately homogeneous exchange field experienced by the quantum-dot electron, the spin-orbit interplay becomes quite weak and a nearly pure spin qubit with the largest Zeeman-like splitting is obtained.

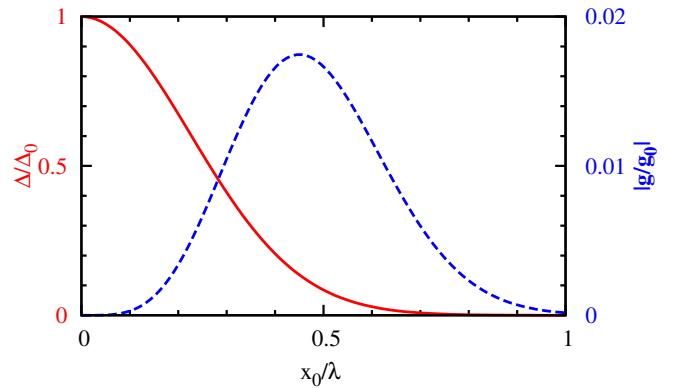


FIG. 2: (Color online) Dimensionless level spacing  $\Delta/\Delta_0$  of the spin-orbit qubit and dimensionless spin-photon coupling  $|g/g_0|$  versus the dimensionless dot size  $x_0/\lambda$ .

#### IV. MODULATION BY THE RASHBA SOC

Although the spin-orbit qubit proposed here is available without employing the Rashba/Dresselhaus SOC, in reality the SOC may be present and even important. Nonetheless, the Rashba SOC is controllable, e.g., by a gate voltage applied to the nanowire [as illustrated by  $V_g$  from the gate electrode on top of the nanowire in Fig. 1(a)]. Below we introduce the Rashba SOC into the nanowire, supplying an effective channel to modulate the spin-orbit qubit as well as its coupling to photons.

With the Rashba SOC included, the Hamiltonian given by Eq. (1) becomes

$$H_\alpha = \frac{p^2}{2m_e} + \frac{1}{2}m_e\omega^2x^2 + \alpha p\sigma_y + \mathbf{J}(x) \cdot \boldsymbol{\sigma}, \quad (9)$$

where  $\alpha$  is the Rashba SOC strength. We now apply the unitary transformation  $\tilde{H}_\alpha = U_\alpha^\dagger(x)H_\alpha U_\alpha(x)$  with  $U_\alpha(x) = \exp(-im_e\alpha x\sigma_y/\hbar)$ , and obtain<sup>16,37</sup>

$$\tilde{H}_\alpha = \frac{p^2}{2m_e} + \frac{1}{2}m_e\omega^2x^2 + \mathbf{J}_\alpha(x) \cdot \boldsymbol{\sigma} + \frac{m_e\alpha^2}{2}, \quad (10)$$

where  $\mathbf{J}_\alpha(x) = J(\sin(\chi q_\alpha x + \phi), 0, \cos(\chi q_\alpha x + \phi))$  with  $q_\alpha = (1 - \alpha/\alpha_0)q$ . The Hamiltonian  $\tilde{H}_\alpha$  has exactly the same form as in Eq. (1). Therefore, one can obtain the low-energy eigenstates of  $\tilde{H}_\alpha$  immediately based on the results given previously. By noting that the electric dipole moment commutes with the unitary operator  $U_\alpha(x)$ , one straightforwardly obtains the level spacing of the spin-orbit qubit and the spin-photon coupling in the presence of the Rashba SOC,

$$\Delta_\alpha = \Delta_0 \exp(-\eta_\alpha^2), \quad (11)$$

$$g_\alpha = g_0(x_0/\lambda)^3 \eta_\alpha \exp(-\eta_\alpha^2), \quad (12)$$

with  $\eta_\alpha = (1 - \alpha/\alpha_0)\eta$ .

The above results can be understood by considering the Rashba SOC to superimpose on the effective Rashba-like SOC from the spiral geometry, or, in other words, to equivalently modulate the wavelength of the spiral magnetic order. This feature allows to control both the level spacing of the spin-orbit qubit and the spin-photon coupling by adjusting the Rashba SOC via the gate voltage. To show the modulation of the Rashba SOC on the hybrid system, in Figs. 3(a, b) we plot the dimensionless level spacing,  $\Delta_\alpha/\Delta_0$ , and dimensionless spin-photon coupling,  $|g_\alpha/g_0|$ , versus the parameters  $x_0/\lambda$  and  $\alpha/\alpha_0$ . Those calculations indicate that when  $x_0 \sim \lambda$  and  $\alpha \sim (1 \pm 0.2)\alpha_0$ , the spin-orbit qubit can be effectively coupled to photons, as indicated by the area near the “on” points in Fig. 3(b). Moreover, by tuning  $\alpha$  to  $\alpha_0$ , the spin-photon coupling is completely switched off due to the decoupling of the spin to the orbit, as indicated by the area near the “off” point in Fig. 3(b). During this switch process, the level spacing of the spin-orbit qubit changes by about 30%. These features are promising for

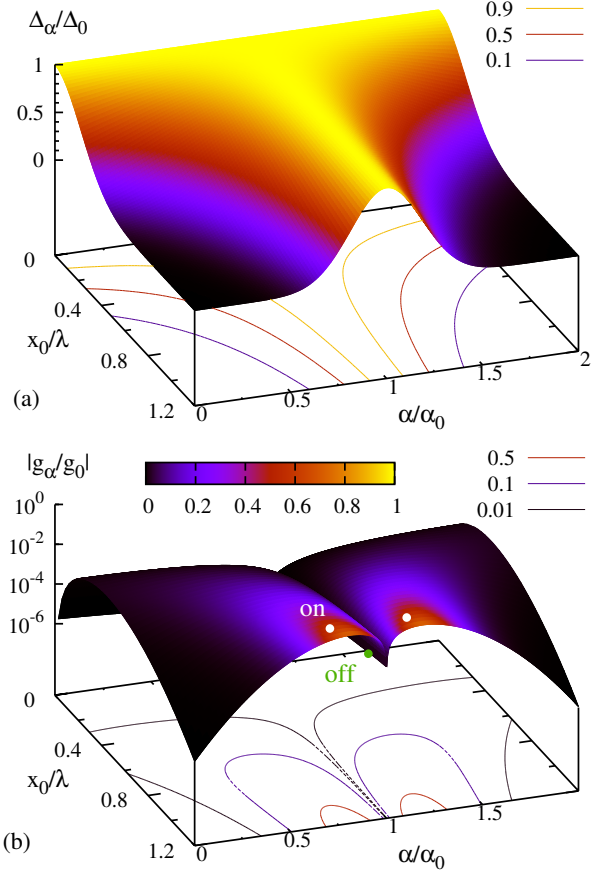


FIG. 3: (Color online) (a) Dimensionless level spacing  $\Delta_\alpha/\Delta_0$  of the spin-orbit qubit and (b) dimensionless spin-photon coupling  $|g_\alpha/g_0|$  (in log-scale) versus  $x_0/\lambda$  and  $\alpha/\alpha_0$ .

manipulating, storing and transferring information in the hybrid quantum systems.<sup>26</sup>

Note that for a particular Rashba SOC, its modulation depends on the spiral helicity in the substrate, as  $\alpha_0$  depends on  $\chi$ . This feature supplies another control channel of the device via the gate voltage  $V_c$  on the substrate, and also in turn provides the possibility to determine the exchange coupling strength  $J$  as well as the Rashba SOC strength  $\alpha$ . By measuring the level spacings of the spin-orbit qubit corresponding to opposite spiral helicities, which satisfy  $\ln[\Delta_\alpha(\chi = 1)/\Delta_\alpha(\chi = -1)] = 2q\alpha/\omega$ , one can obtain the Rashba SOC strength  $\alpha$  with the knowledge of the confining potential of the quantum dot. Here  $\alpha$  is assumed to be marginally affected by the reversal of the spiral helicity. Further, the exchange coupling strength  $J$  is available based on the known  $\Delta_\alpha$  and  $\alpha$ .

#### V. EXPERIMENTAL REALIZABILITY

Let us now discuss the experimental realizability of the proposed spin-orbit qubit and its coupling to the superconducting coplanar waveguide. We consider a  $\langle 110 \rangle$ -

oriented Ge nanowire<sup>39–41</sup> on the surface of the multiferroic insulator BiFeO<sub>3</sub>.<sup>31,34,36</sup> In the ⟨110⟩-oriented Ge nanowire, the electron effective mass  $m_e = 0.08m_0$ , where  $m_0$  is the free electron mass.<sup>41</sup> For BiFeO<sub>3</sub>, the wavelength of the spiral magnetic order  $\lambda = 62$  nm,<sup>31,36</sup> while the magnon frequency is of the order of 100 GHz.<sup>35</sup> The exchange coupling strength is set as  $J = 5$   $\mu$ eV, smaller than the estimated interface exchange coupling (16  $\mu$ eV) induced by the ferromagnetic-insulator contacts in Ref. 23. The electric field in the superconducting coplanar waveguide has the typical maximal strength<sup>15</sup>  $E = 0.2$  V/m. With these parameters, we have  $\Delta_0 = (2\pi)2.4$  GHz,  $|g_0| = (\pi)0.1$  MHz, and  $|\alpha_0| = 7.4 \times 10^4$  m/s. Moreover, even when  $x_0 \sim \lambda$ , the orbital splitting in the quantum dot is  $\hbar\omega \sim 0.25$  meV, still much larger than the exchange coupling strength  $J$ . In addition to the availability of an effective spin-photon coupling with an efficient on/off switching, the proposed device has another advantage. That is, in isotopically-purified <sup>72</sup>Ge samples, the hyperfine interaction can be markedly suppressed and hence the coherence time of the spin-orbit qubit in the zero-temperature limit can be quite long.<sup>15</sup> This feature benefits the application of the proposed device.

## VI. CONCLUSION

In conclusion, we have proposed a spin-orbit qubit based on a nanowire quantum dot on the surface of a multiferroic insulator, and designed a hybrid quantum circuit by integrating this spin-orbit qubit into a super-

conducting coplanar waveguide.

The spiral exchange field from the magnetic moments in the multiferroic insulator causes an inhomogeneous Zeeman-like interaction on the electron spin in the quantum dot. This effect assists the realization of a spin-orbit qubit in the quantum dot. In this approach, no external magnetic field is employed, benefitting the on-chip fabrication of the spin-orbit qubit in a superconducting coplanar waveguide. Our study reveals that both the level spacing of the spin-orbit qubit and the spin-photon coupling are proportional to the exchange coupling strength and depend on the ratio of the dot size to the wavelength of the spiral magnetic order. We further consider the effect of the Rashba SOC, which is controllable by a gate voltage on the nanowire. It is found that by invoking the Rashba SOC, one is able to obtain an effective spin-photon coupling with an efficient on/off switching, making the device promising for applications. The proposed spin-orbit qubit may be experimentally realizable by placing a ⟨110⟩-oriented Ge nanowire on the surface of the multiferroic insulator BiFeO<sub>3</sub>.

## Acknowledgments

The authors gratefully acknowledge E. Ya. Sherman and X. Hu for valuable discussions and comments. F.N. is partially supported by the ARO, RIKEN iTHES Project, MURI Center for Dynamic Magneto-Optics, JSPS-RFBR contract No. 12-02-92100, Grant-in-Aid for Scientific Research (S), MEXT Kakenhi on Quantum Cybernetics, and the JSPS via its FIRST program.

---

<sup>1</sup> D. Loss and D. P. DiVincenzo, Phys. Rev. A **57**, 120 (1998).  
<sup>2</sup> R. Hanson, J. R. Petta, S. Tarucha, and L. M. K. Vandersypen, Rev. Mod. Phys. **79**, 1217 (2007).  
<sup>3</sup> M. W. Wu, J. H. Jiang, and M. Q. Weng, Phys. Rep. **493**, 61 (2010).  
<sup>4</sup> I. Buluta, S. Ashhab, and F. Nori, Rep. Prog. Phys. **74**, 104401 (2011).  
<sup>5</sup> F. A. Zwanenburg, A. S. Dzurak, A. Morello, M. Y. Simmons, L. C. L. Hollenberg, G. Klimeck, S. Rogge, S. N. Coppersmith and M. A. Eriksson, Rev. Mod. Phys. **85**, 961 (2013).  
<sup>6</sup> H. A. Engel and D. Loss, Phys. Rev. Lett. **86**, 4648 (2001).  
<sup>7</sup> F. H. L. Koppens, C. Buizert, K. J. Tielrooij, I. T. Vink, K. C. Nowack, T. Meunier, L. P. Kouwenhoven, and L. M. K. Vandersypen, Nature **442**, 766 (2006).  
<sup>8</sup> D. D. Awschalom, L. C. Bassett, A. S. Dzurak, E. L. Hu, and J. R. Petta, Science **339**, 1174 (2013).  
<sup>9</sup> E. I. Rashba and Al. L. Efros, Phys. Rev. Lett. **91**, 126405 (2003).  
<sup>10</sup> E. I. Rashba, J. Supercond. **18**, 137 (2005).  
<sup>11</sup> V. N. Golovach, M. Borhani, and D. Loss, Phys. Rev. B **74**, 165319 (2006).  
<sup>12</sup> K. C. Nowack, F. H. L. Koppens, Y. V. Nazarov, and L. M. K. Vandersypen, Science **318**, 1430 (2007).  
<sup>13</sup> S. N. Perge, V. S. Pribiag, J. W. G. van den Berg, K. Zuo, S. R. Plissard, E. P. A. M. Bakkers, S. M. Frolov, and L. P. Kouwenhoven, Phys. Rev. Lett. **108**, 166801 (2012).  
<sup>14</sup> D. V. Khomitsky, L. V. Gulyaev, and E. Ya. Sherman, Phys. Rev. B **85**, 125312 (2012).  
<sup>15</sup> X. Hu, Y. X. Liu, and F. Nori, Phys. Rev. B **86**, 035314 (2012).  
<sup>16</sup> R. Li, J. Q. You, C. P. Sun, and F. Nori, Phys. Rev. Lett. **111**, 086805 (2013).  
<sup>17</sup> A. F. Sadreev and E. Ya. Sherman, Phys. Rev. B **88**, 115302 (2013).  
<sup>18</sup> C. Echeverría-Arrondo and E. Ya. Sherman, Phys. Rev. B **88**, 155328 (2013).  
<sup>19</sup> Y. Kato, R. C. Myers, D. C. Driscoll, A. C. Gossard, J. Levy, and D. D. Awschalom, Science **299**, 1201 (2003).  
<sup>20</sup> Y. Tokura, W. G. van der Wiel, T. Obata, and S. Tarucha, Phys. Rev. Lett. **96**, 047202 (2006).  
<sup>21</sup> M. Pioro-Ladrière, T. Obata, Y. Tokura, Y. S. Shin, T. Kubo, K. Yoshida, T. Taniyama, and S. Tarucha, Nat. Phys. **4**, 776 (2008).  
<sup>22</sup> T. Obata, M. Pioro-Ladrière, Y. Tokura, Y. S. Shin, T. Kubo, K. Yoshida, T. Taniyama, and S. Tarucha, Phys. Rev. B **81**, 085317 (2010).

<sup>23</sup> A. Cottet and T. Kontos, Phys. Rev. Lett. **105**, 160502 (2010).

<sup>24</sup> E. A. Laird, C. Barthel, E. I. Rashba, C. M. Marcus, M. P. Hanson, and A. C. Gossard, Phys. Rev. Lett. **99**, 246601 (2007).

<sup>25</sup> M. Shafiei, K. C. Nowack, C. Reichl, W. Wegscheider, and L. M. K. Vandersypen, Phys. Rev. Lett. **110**, 107601 (2013).

<sup>26</sup> Z. L. Xiang, S. Ashhab, J. Q. You, and F. Nori, Rev. Mod. Phys. **85**, 623 (2013).

<sup>27</sup> J. Q. You and F. Nori, Physics Today **58**, 42 (2005); Nature **474**, 589 (2011).

<sup>28</sup> N. Lambert, C. Flindt, F. Nori, Euro. Phys. Lett. **103**, 17005 (2013).

<sup>29</sup> G. Burkard and A. Imamoglu, Phys. Rev. B **74**, 041307 (2006).

<sup>30</sup> P. Q. Jin, M. Marthaler, A. Shnirman, and G. Schön, Phys. Rev. Lett. **108**, 190506 (2012).

<sup>31</sup> D. Lebeugle, D. Colson, A. Forget, M. Viret, P. Bonville, J. F. Marucco, and S. Fusil, Phys. Rev. B **76**, 024116 (2007).

<sup>32</sup> T. Kimura, Annu. Rev. Mater. Res. **37**, 387 (2007).

<sup>33</sup> Y. Yamasaki, H. Sagayama, T. Goto, M. Matsuura, K. Hirota, T. Arima, and Y. Tokura, Phys. Rev. Lett. **98**, 147204 (2007).

<sup>34</sup> D. Khomskii, Physics **2**, 20 (2009).

<sup>35</sup> P. Rovillain, R. de Sousa, Y. Gallais, A. Sacuto, M. A. Méasson, D. Colson, A. Forget, M. Bibes, A. Barthélémy, and M. Cazayous, Nat. Mater. **9**, 975 (2010).

<sup>36</sup> R. Thomas, J. F. Scott, D. N. Bose, and R. S. Katiyar, J. Phys.: Condens. Matter **22**, 423201 (2010).

<sup>37</sup> P. Zhang and M. W. Wu, Phys. Rev. B **84**, 014433 (2011).

<sup>38</sup> F. Zhai and P. Mu, Appl. Phys. Lett. **98**, 022107 (2011).

<sup>39</sup> Y. Wu and P. Yang, J. Am. Chem. Soc. **123**, 3165 (2001).

<sup>40</sup> A. B. Greytak, L. J. Lauhon, M. S. Gudiksen, and C. M. Lieber, Appl. Phys. Lett. **84**, 4176 (2004).

<sup>41</sup> Y. M. Niquet and C. Delerue, J. Appl. Phys. **112**, 084301 (2012).